

# Surface Modification of Precipitated Calcium Carbonate(PCC)-Derived From Indonesia's Limestone using Sodium Tripolyphosphate and Sodium Stearic

Sri Wardhani <sup>1,\*</sup>, Rendy Muhamad Iqbal <sup>2,3,4</sup>, Darjito Darjito <sup>1</sup>, Davina Kurniasari <sup>1</sup>, Shafira Qurrota Ayuningtyas <sup>1</sup>

<sup>1</sup> Department of Chemistry, Faculty of Mathematics and Natural Science, Brawijaya University, Malang 65145, Indonesia

<sup>2</sup> Department of Chemistry, Faculty of Mathematic and Natural Science, Universitas Palangka Raya, Palangka Raya 73111, Indonesia

<sup>3</sup> Department of Chemistry, Faculty of Science, Universiti Teknologi Malaysia, Skudai 81310, Johor Bahru, Malaysia

<sup>4</sup> Advanced Membrane Technology Research Center, Faculty of Chemical and Energy Engineering, Universiti Teknologi Malaysia, Skudai 81310, Johor Bahru, Malaysia

\* Correspondence: wardhani@ub.ac.id;

Scopus Author ID 57201862647

Received: 13.06.2023; Accepted: 16.11.2023; Published: 20.07.2024

**Abstract:** Limestone is an abundant natural resource in Indonesia that can be utilized to synthesize PCC (precipitated calcium carbonate). This study aimed to modify the PCC surface using Sodium Tripolyphosphate (NaTPP) and Sodium Stearic (Sodium stearic) as the modifier. PCC was successfully synthesized using the caustic soda method. Firstly, limestone was calcined at 900°C, the solid powder was immersed into 6M of HNO<sub>3</sub>, and 1 M of Na<sub>2</sub>CO<sub>3</sub> was added to the mixture. The PCC in this study was modified with Sodium Tripolyphosphate and Sodium Stearic; then, the solid powders were characterized by XRD, FTIR, and Water Contact Angle (WCA). Based on the results of the AAS characterization, limestone contains 45.87% of calcium carbonate, and PCC-NaTPP contains 80% of calcium carbonate. Characterization using contact angle resulted in a contact angle of 128° at PCC-NaTPP with the addition of 4% Sodium stearic and a reaction temperature of 60°C. Characterization using FTIR marked the phosphate functional group from the addition of NaTPP and the C=O functional group caused by fatty acids from sodium stearic. XRD pattern of PCC represents the successful transformation from the dolomite phase to calcite, which refers to the CaCO<sub>3</sub> structure. Then, the higher contact angle obtained with sodium stearic modification leads to the lower surface free energy.

**Keywords:** precipitated calcium carbonate; NaTPP; sodium stearic; hydrophobic.

© 2024 by the authors. This article is an open-access article distributed under the terms and conditions of the Creative Commons Attribution (CC BY) license (<https://creativecommons.org/licenses/by/4.0/>).

## 1. Introduction

The existence of limestone in Indonesia as a mineral resource is very abundant; the amount is estimated to be around 2,160 billion tons. The deposits are known to be spread over various islands such as Sumatra, Java, Nusa Tenggara, Sulawesi, Papua, and other islands in Indonesia. In the industrial sector, limestone and its derivate products have been widely used in various fields, such as an additive in the metal smelting industry, both ferrous and non-ferrous and the glass industry; filler material in the manufacture of rubber, plastic, cardboard, paint, toothpaste, and other products [1-2]. Limestone can also be used as a source for the synthesis of calcium carbonate (CaCO<sub>3</sub>) [3].

Calcium carbonate is available in two forms: soil calcium carbonate (GCC), which is produced through the grinding process of calcium carbonate mining, such as marble and limestone, and precipitated calcium carbonate (PCC) is produced through carbonation or a special precipitation process [4]. PCC can also be synthesized from limestone by three methods: carbonation [5], caustic soda [6], and Solvay [7]. Azkiyah et al. [6] successfully synthesized PCC with the caustic soda method; it starts from the calcination process to transform limestone to form CaO. Then, CaO powder dissolved in water to form Ca(OH)<sub>2</sub>, which is then reacted with Na<sub>2</sub>CO<sub>3</sub> to form CaCO<sub>3</sub> (PCC) [8–10]

PCC synthesis can have different morphology by varying several process parameters such as temperature, total dissolved calcium concentration, CO<sub>2</sub> flow rate, the mass concentration of Ca(OH)<sub>2</sub>, and the rate of Ca(OH)<sub>2</sub> addition [7,11,12]. Research on the morphological control of CaCO<sub>3</sub> has been actively sought. The hydrophilic characteristics can be formed by the increase in the atomization of the PCC powder; it can also increase the diffusion energy on the PCC surface, which can cause low dispersion and agglomeration when mixed in an organic polymer matrix. Therefore, the use of PCC as a filler material may experience limitations due to its irregular surface and low adhesive force. The surface modification of PCC hydrophobic was carried out to overcome this problem by modifying the physical properties by transforming the surface properties to increase the solubility of the polymer matrix and reduce the surface tension. Its purpose is to improve the physical properties, mechanical performance, thermal resistance, or dispersibility [11–13]

Hydrophobic PCC has many benefits in industrial applications. Hydrophobic PCC has superior properties as a filler for paper, mortar, and concrete. Hydrophobic PCC can be made using oleic acid, stearic acid, or dodecanoic acid (long-chain fatty acid group) [5, 14]. Stearic acid is a surfactant to make hydrophobic PCC [15–17]. The synthesis of PCC nanoparticles using stearic acid obtained better dispersion properties and helped improve the mechanical properties of the polymer.

In addition, sodium stearic (Na-stearic) can be used as a surfactant to make hydrophobic PCC [18]. Tran et al. [18] reported that the contact angle increased significantly with Na-stearic content of 0.3-5%. Tang et al. [19] reported that the increasing concentration of sodium stearic could increase the hydrophobicity of the material due to the higher amount of stearic molecule, which can be adsorbed on the material's surface. On the other hand, Wang et al. [20] found that temperature affects the interaction between organic substrates and CaCO<sub>3</sub>, an increase of the active ratio as the temperature increases, thereby increasing the hydrophobicity. This study aims to observe the effect of the stearic molecule on the surface properties of CaCO<sub>3</sub> derived from Indonesian limestone with some parameters such as reaction time, concentration, and reaction temperature, as well as its effects on the surface properties of PCC.

## 2. Materials and Methods

### 2.1. Materials.

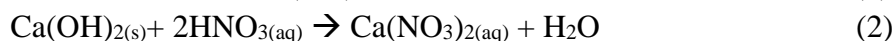
The limestone was collected from Tuban, East Java Province, Indonesia. The other materials used in this work were HNO<sub>3</sub> (Aldrich, 70%), Na<sub>2</sub>CO<sub>3</sub> (Aldrich, 99.5%), Sodium Tripolyphosphate (Merck, 85%), and Sodium Stearic (Aldrich, 99%).

## 2.2. Preparation of limestone.

Firstly, the limestone is ground and crushed. After that, the limestone was sieved with a 150-mesh sieve. Fine powder of limestone was calcined at 900°C for 30 minutes. Then, the lime powder was destroyed by aqua regia and followed by an AAS measurement to determine the Ca content.

## 2.3. Synthesis of precipitated calcium carbonate(PCC) using caustic soda method.

CaO from limestone samples was used as a calcium precursor, and Na<sub>2</sub>CO<sub>3</sub> was used as a carbonate precursor. Initially, limestone samples were reacted with distilled water to produce a Ca(OH)<sub>2</sub>Ca(OH)<sub>2</sub> suspension suspension, and 6.02M of HNO<sub>3</sub> was added. This was followed by adding 1M Na<sub>2</sub>CO<sub>3</sub> to form CaCO<sub>3</sub>. At this stage, 1M Na<sub>2</sub>CO<sub>3</sub> was added to the Ca<sup>2+</sup> solution until it reached pH 8. The precipitated calcium carbonate (PCC) was then washed with distilled water until the pH was neutral. After that, the PCC was filtered and dried at 100°C for 4 hours. The mechanism of the reaction was shown in equations 1-3.



## 2.4. Surface modification of PCC using NaTPP.

11.2 grams of calcined lime was added with 200 mL of distilled water. The mixture was then added with 40mL of 6M HNO<sub>3</sub> solution while stirring at a stirring speed of 700rpm, which was carried out in a fume hood accompanied by heating at 65°C for 30 minutes. The mixture was then filtered, and the filtrate obtained was added with 4mL of 1% sodium tripolyphosphate. After that, 1M Na<sub>2</sub>CO<sub>3</sub> was added to pH 8-9 while stirring at 350rpm for 60 minutes. Then, the powder was dried at 100°C for 4 hours.

## 2.5. Effect of reaction time.

The dried PCC-modified NaTPP (PCC-NaTPP) was taken 1g and added into sodium stearic with variations of 1.5, 2, 2.5, 3, and 3.5%. It was stirred at 200rpm for different reaction times, such as 15, 30, 45, 60, and 75 minutes. After that, the mixture was added with 20mL of distilled water and filtered to separate the precipitated powder. The resulting precipitate powder was dried at 100°C for 4 hours. The solid powder was characterized using Contact Angle Analysis (CAA), XRD PANalytical type X'Pert3, FTIR Shimadzu 84000S, and Particle Size Analyzer Cilas 1090. For the contact angle analysis, the fine powder was pressed to form a pellet; then characterized using CAA.

## 2.6. Effect of sodium stearic concentration and reaction temperature.

1 gram of PCC-NaTPP was mixed into 100mL of distilled. The mixture was then added with sodium stearic with various concentrations (3; 3,5; 4; 4,5; and 5%); it was stirred at 200rpm and reacted with temperature variations (25, 40, 60, 80, and 100°C) for 45 minutes. The precipitate obtained was filtered and dried at 100°C for 4 hours. After that, the precipitate was characterized by CAA.

### 2.7. Determination of surface free energy.

After the contact angle data obtained by this experiment, the surface free energy was also determined using the Young equation, which established:

$$\gamma_{sl} = \gamma_s - \gamma_l \cos\theta \quad (4)$$

$$\gamma_{sl} = \gamma_s + \gamma_l - 2(\gamma_s \gamma_l)^{1/2} \quad (5)$$

From the equations of (4) and (5), it can form equation (6) as follow :

$$\gamma_s = \gamma_l (1 + \cos\theta)^2 / 4 \quad (6)$$

Where  $\theta$  is the contact angle value,  $\gamma_{sl}$  is interfacial free energy between solid and liquid,  $\gamma_l$  is the surface free energy of liquid. In this work, we used water as a liquid; its value is 72.8 mJ/m<sup>2</sup>, then  $\gamma_s$  is surface free energy from a solid.

## 3. Results and Discussion

### 3.1. Ca content in natural limestone.

AAS was measured to determine the percentage of calcium ions and the percentage of calcium carbonate contained in limestone. This measurement used a wavelength of Ca 422.7nm. Based on the results of this measurement, the calcium content was 18.35%, and calcium carbonate was 45.87%. In PCC-NaTPP, the calcium content was 32.055%, and the calcium carbonate was 80%.

### 3.2. XRD characterization.

The results of the diffractogram spectra from this characterization are shown in Figure 1. The crystal phase of the limestone samples analyzed is dolomite. The dolomite structure represented by 2 theta of 30.95, 33.54, 37.37, 41.14, 44.94, 50.93, and 51.07° which is suitable with JCPDS PDF no. 96-151-7791 (CaMgC<sub>2</sub>O<sub>6</sub> or Dolomite) The dolomite was successfully transformed to be another phase after PCC synthesis. In Figure 1, the crystalline phases of PCC are identified in the form of calcite at 2 theta of 23.16, 29.56, 36.13, 39.59, 43.34, 47.77, 48.76, and 57.65°. It was suitable for JCPDS PDF no 96-900-9669 (calcite). Calcite represents the structure of CaCO<sub>3</sub>. The crystal size of PCC calculated using modified Scherrer equations obtained a crystal size of 48.53nm. Its size is smaller than the result reported by Tran [18]; the crystal size was 65nm.

### 3.3. FTIR characterization.

The FTIR spectra of the synthesized and modified PCC samples are presented in Figure 2. The interpretation data of the wavenumber is presented in Table 1. The FTIR spectrum of the PCC sample with the addition of NaTPP has three strong peaks at wavenumbers such as 1424.79cm<sup>-1</sup>, 875.69cm<sup>-1</sup>, and 714.53cm<sup>-1</sup>, which indicate the presence of vibrations from the carbonate functional group. At a wavenumber of 3442.87cm<sup>-1</sup>, a wide and weak peak is caused by the presence of the O-H functional group. The vibration of 1799.88cm<sup>-1</sup> represents the presence of C=O from carbonate. Another functional group at a wave number of 1086.77cm<sup>-1</sup> indicates the presence of a phosphate group from the addition of NaTPP.

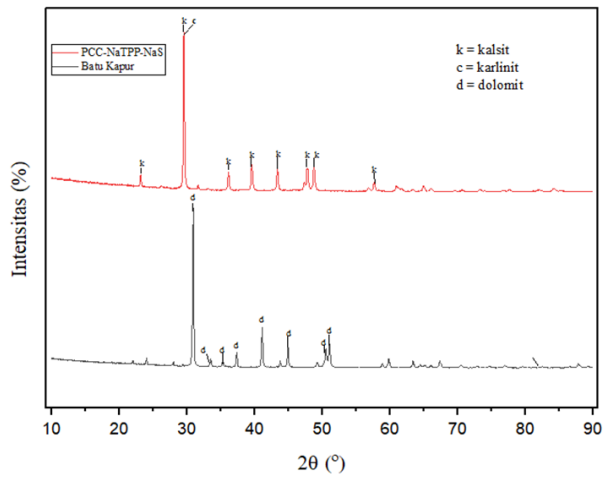


**Figure 1.** XRD Pattern of Indonesia's Limestone and PCC-NaTPP-Sodium stearic.

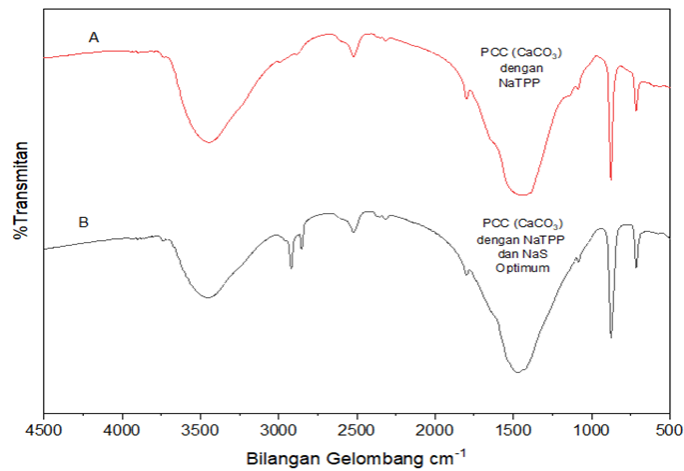


**Figure 2.** FTIR spectra of PCC-NaTPP and PCC-NaTPP-Sodium Stearic.

**Table 1.** Interpretation of FTIR Spectra.

Wavenumber (cm <sup>-1</sup> )		Molecular Vibration
PCC-NaTPP	PCC- NaTPP-Sodium stearic	
3442.87	3450.01	O-H
-	2919.46	C-H
-	2851.00	C-C
2520.12	2520,12	C-C
1798.45	1799.88	C=O
1424.79	1473.28	C-O
1086.77	1082.49	P=O
875.69	874.27	C-O
714.53	713.11	C-O

FTIR spectrum of the PCC-NaTPP with the addition of sodium stearic has a new peak that appears compared to PCC-NaTPP, at the peak of 2851cm<sup>-1</sup>, indicating the presence of symmetrical and asymmetrical vibration of C-C, which means sodium stearic has been adsorbed or grafted on the CaCO<sub>3</sub> surface. At the peak of 1473.28cm<sup>-1</sup>, there is a shift in the peak of the IR spectrum, which indicates the chemical absorption of sodium stearic on the PCC surface. The molecular vibration at 1473.28, 874.27, and 713.11cm<sup>-1</sup> showed the presence of a carbonate group from PCC. At wavenumbers 3450.01cm<sup>-1</sup>, 2919.46cm<sup>-1</sup>, and 2851.00cm<sup>-1</sup>, the presence of functional groups O-H, C-H, and C-C, respectively, was found. It exhibits the presence of ionized carboxylic acid functional groups from the addition of sodium stearic. At the wavenumber of 1082.49cm<sup>-1</sup>, a phosphate functional group was found from the addition of

NaTPP. At a wavenumber of  $1799.88\text{cm}^{-1}$ , it represents the C=O functional group caused by the presence of fatty acids from sodium stearic. This indicated that the PCC surface modification with the addition of NaTPP and sodium stearic was successful.

*3.4. Effect of reaction time on surface properties.*

Figure 3 shows the effect of reaction time on the contact angle of PCC-NaTPP-Sodium Stearic. PCC-NaTPP with 3.5% sodium stearate produced the largest contact angle value ( $87.9^\circ$ ), close to  $90^\circ$ . Based on Figure 3, the increasing reaction time increases the contact angle from  $70.2^\circ$  to  $87.9^\circ$  and decreases slowly to  $72.7^\circ$ . Increasing the reaction time conditioned sodium stearic to be adsorbed onto the PCC surface. However, if the reaction time is extended continuously, the contact angle will decrease because the solution has reached a saturated state [21–23]. At 45 minutes of reaction time, the contact angle on the PCC surface reached the optimum value and slowly decreased when the reaction time was 60 and 75 minutes. The droplet water on PCC-NaTPP-sodium stearic was shown in Figure 4; the reaction time of 15, 30, 45, 60, and 75 minutes was denoted as A, B, C, D, and E, respectively. Then, the sodium stearic concentrations of 1.5, 2, 2.5, 3, and 3.5% were denoted as codes of 1, 2, 3, 4, and 5, respectively.

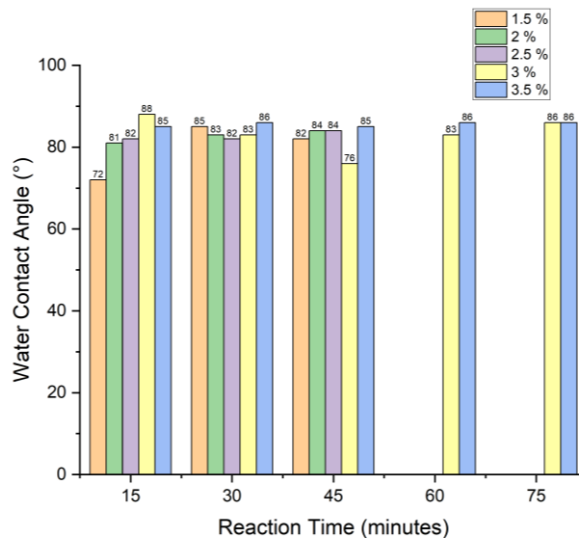


**Figure 3.** The effect of reaction time on the contact angle of PCC-NaTPP-Sodium Stearic.

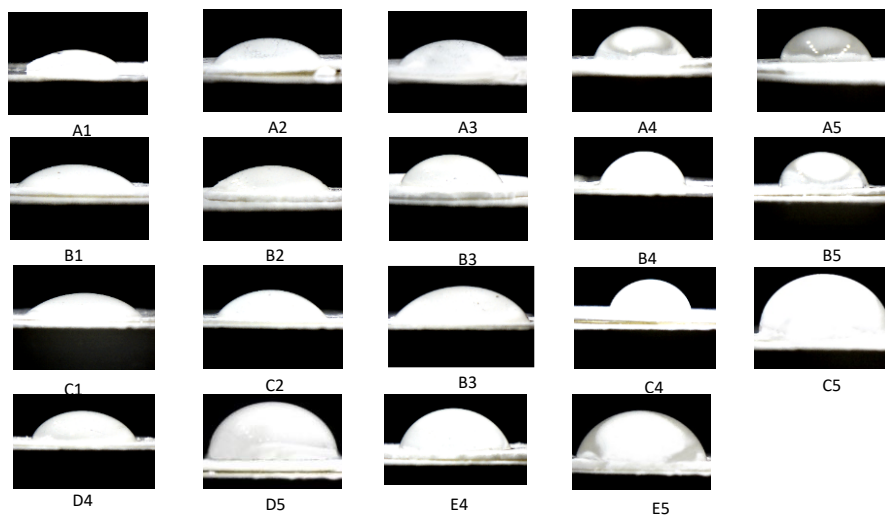


**Figure 4.** Droplet water of PCC-NaTPP-Sodium Stearic with different reaction times.

Surface free energy (SFE) was determined in this study as follows Young equation. As can be seen in Figure 5, the sodium stearic concentration of 3.5% obtained the lower surface free energy in all reaction times. It can be influenced by the amount of stearic molecule successfully adsorbed or grafted on the surface PCC-NaTPP, then it obtained the higher contact angle compared to other samples. Contact angle directly influenced SFE value; the higher contact angle leads to decreased surface free energy.

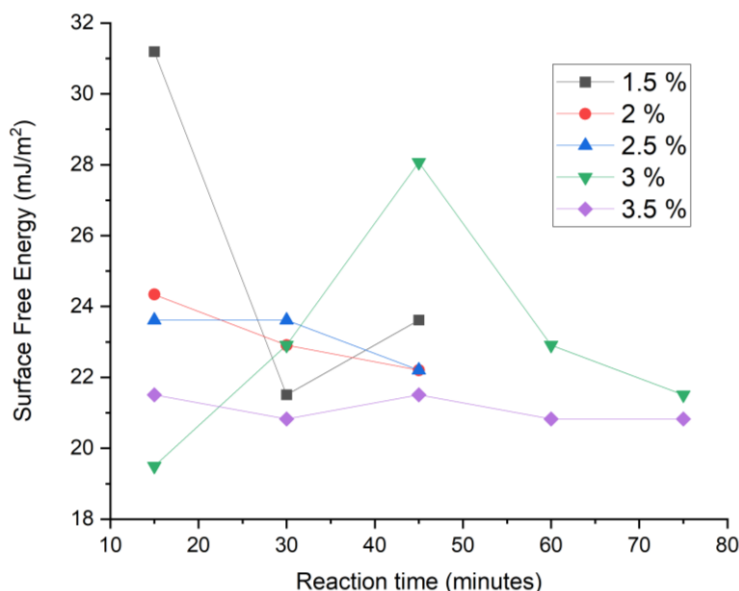


**Figure 5.** Surface free energy of PCC-NaTPP-Sodium Stearic with different reaction times.

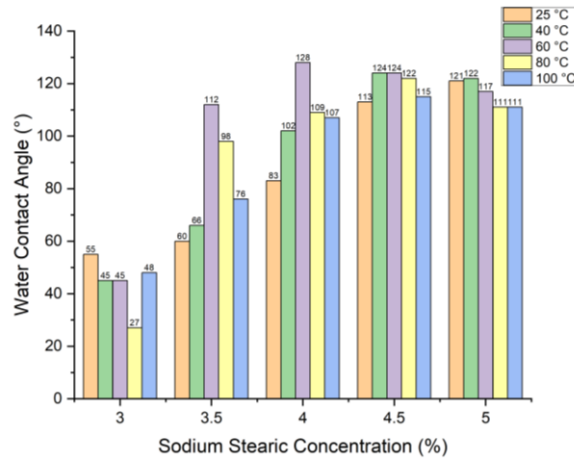
### 3.5. Effect of sodium stearic concentration on surface properties.

This research was conducted to determine the effect of sodium stearic concentration on the hydrophobic properties of PCC. Therefore, the contact angle measurement was carried out to determine the hydrophobicity of the modified PCC. In this study, 5 variations of sodium stearic concentration and 5 variations of reaction temperature were carried out to obtain 25 contact angles data; in addition, measuring the contact angle for PCC with sodium triphosphate modifier as a control obtained a contact angle of 9.3°.

The surface properties of a sample can be concluded to be hydrophobic if it has a contact angle above 90° and superhydrophobic if it has a contact angle above 150° [24]. PCC contact angle without the addition of sodium stearic, the sample's surface is still hydrophilic because it produces a contact angle below 90°.

The effect of surfactant concentration on hydrophobicity has been widely developed, one of them by Liang et al. [25]. In his research, the contact angle increased with the addition of sodium stearic concentration. Another study by Ukrainczyk et al. [26] found that adding sodium stearic concentration will increase the contact angle. In this study, the sample's surface has been coated with stearic ions. In Figure 6, the Sodium stearic concentration of 3% significantly impacts the surface properties' transformation. Then, the concentration of 4% Sodium Stearic with a reaction temperature of 60°C became the optimum condition in this study because it produced the largest contact angle with a contact angle of 128°. These results follow the research conducted by Wang et al. [20] with the optimal temperature of 60°C. The decrease in temperature above 90°C can be caused by the surface roughness of the sample, which considerably influences decreasing the contact angle.

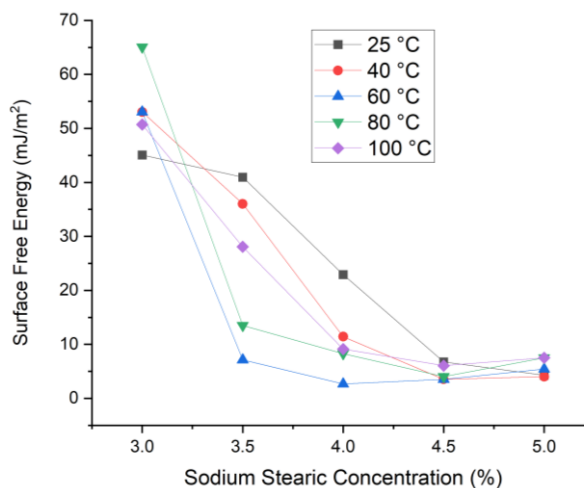
In the concentration range of 3.5 - 4%, there was a sharp increase in the contact angle up to a reaction temperature of 60°C, which was followed by a decrease in the contact angle at 80 and 100°C. At a concentration of 4.5%, the increase of contact angle occurs in a narrow range up to a temperature of 40°C and tends to be constant up to a temperature of 60°C, then decreases at a temperature of 80 and 100°C.



**Figure 6.** The effect of sodium stearic contraction on the contact angle of PCC-NaTPP-Sodium Stearic.

At a concentration of 5%, the increase of contact angle only occurs until the reaction temperature is 40 °C and decreases at the above temperature. Shin et al. [15] mentioned that excessive use of surfactants will cause the formation of a bilayer and the presence of free acid molecules, reducing the value of the contact angle. The contact angle can be influenced by several factors, such as chemical structure [27], surface smoothness [28], pores filled with water [16], and the presence of impurities [29,30]. The droplet water on PCC-NaTPP-sodium stearic with different concentrations is shown in Table 2.

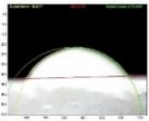
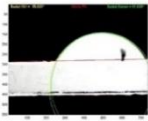
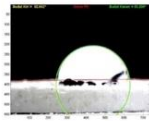
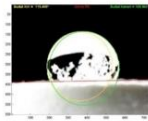
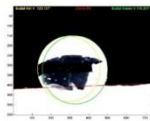
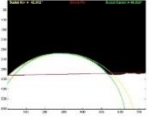
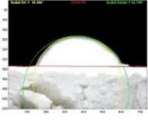
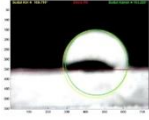
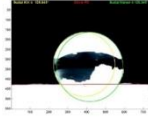
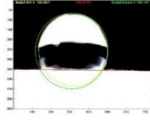
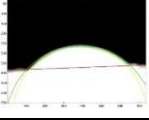
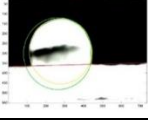
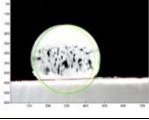
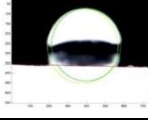
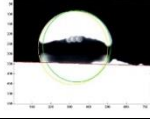
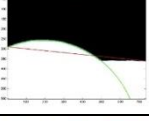
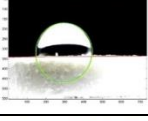
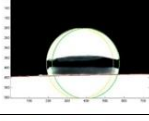
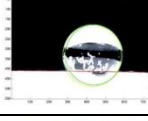
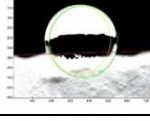
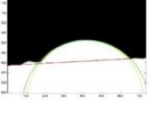
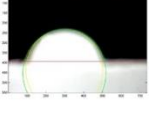
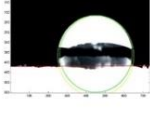
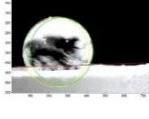
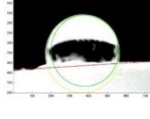
Another surface parameter that is important to observation is surface free energy. The surface free energy (SFE) result is shown in Figure 7. The SFE has an opposite trend with the contact angle. The higher the contact angle obtained, the lower the surface free energy of the materials. As shown in Figure 7, the higher concentration of sodium stearic as a modifier obtained a lower surface free energy; conversely, the lower concentration of sodium stearic obtained a higher surface free energy.



**Figure 7.** Surface free energy PCC-NaTPP-Sodium Stearic with different concentrations.



**Table 2.** The water droplets on the surface PCC-NaTPP-Sodium Stearic with different concentrations.

Temperature (°C)	3 %	3.5 %	4 %	4.5 %	5 %
25					
40					
60					
80					
100					

3.6. Particle size measurement.

The effect of reaction time on the particle size of PCC-NaTPP-sodium stearic was obtained based on analysis with PSA. PSA allows each particle to be analyzed, so it can ensure the distribution of particles with high precision. PSA was carried out on 3.5% PCC-NaTPP-sodium stearic with variations in reaction time (15-75 minutes). In Table 3, it can be seen that the measurement results of the 3.5% PCC-NaTPP-sodium stearic sample for the variation in reaction time were that the largest diameter size is owned by PCC-NaTPP-sodium stearic 3.5% with a reaction time of 60 minutes, at 10% diameter of 1.91µm, at 50% diameter of 11.50µm and 90% diameter of 24.34µm. The smallest particle diameter size was owned by PCC-NaTPP-sodium stearic 3.5% with a reaction time of 15 minutes, at 10% diameter of 1.21µm, at 50% diameter of 6.02µm, and 90% diameter of 21.00µm. These data show that the reaction time has a correlation that is directly proportional to the particle diameter size, where the longer the reaction time, the larger the diameter of the resulting particle. The longer reaction time leads to an increase in particle growth with a narrow size distribution so that more modifiers adhere and cause a large size. However, when the reaction time was longer than 60 min, the particle diameter was not larger than 12.58µm.

**Table 3.** The particle size measurement result.

Reaction time (minutes)	Diameter of 10% (µm)	Diameter of 50% (µm)	Diameter of 90% (µm)	Average diameter (µm)
15	1.21	6.02	21.00	9.41
30	1.27	7.15	21.35	9.92
45	1.36	8.29	21.44	10.36
60	1.91	11.50	24.34	12.58
75	1.76	10.09	21.80	11.22

## 4. Conclusions

PCC was successfully synthesized using the caustic soda method from Indonesia limestone, and its surface can be transformed into hydrophobic using NaTPP and sodium stearic as a modifier. Based on the diffractogram, the PCC has a calcite phase, representing the formation of  $\text{CaCO}_3$ . Then, the FTIR spectrum of PCC-NaTPP-sodium stearic confirmed the presence of C-C and C-H vibration at  $2,851$  and  $2,919.46\text{cm}^{-1}$ , which indicates stearic molecules, it can be concluded that the stearic molecules were successfully adsorbed/grafted on the surface of PCC. The highest contact angle of PCC modification is  $128^\circ$  for PCC-NaTPP with the addition of 4% Sodium stearic and a reaction temperature of  $60^\circ\text{C}$ . The higher the contact angle obtained, the lower the surface free energy of materials.

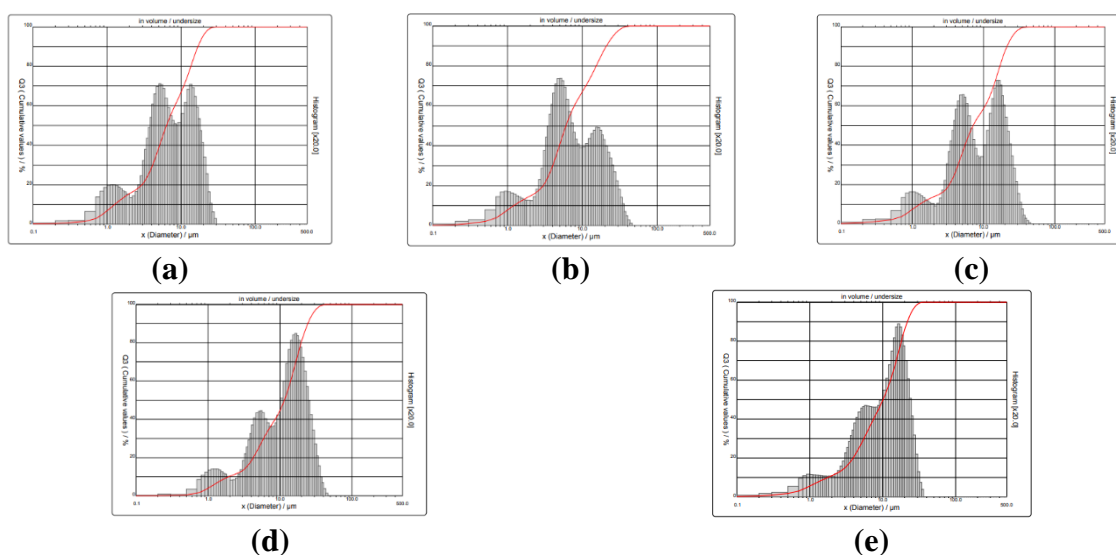


**Figure 8.** Histogram PSA of PCC-NaTPP-sodium stearic with the concentration of 3.5% at different reaction times: (a) 15; (b) 30; (c) 45; (d) 60; (e) 75 minutes.

## Funding

This research was funded by the Faculty of Mathematic and Natural Sciences of Brawijaya University under DPP/SPP research grant scheme with contract no 11/UN10.F09.1/PN/2020

## Acknowledgments

The author thanks the Laboratory of Inorganic Chemistry, Department of Chemistry, Brawijaya University, for providing research facilities and the Department of Physics, Brawijaya University, for the contact angle facility.

## Conflicts of Interest

The authors declare no conflict of interest.

## References

1. Xu, X.; Guo, H.; Li, M.; Deng, X. Bio-cementation improvement via  $\text{CaCO}_3$  cementation pattern and crystal polymorph: A review. *Constr. Build. Mater.* **2021**, *297*, 123478, <http://doi.org/10.1016/j.conbuildmat.2021.123478>.
2. Yadav, V.K.; Yadav, K.K.; Cabral-Pinto, M.M.S.; Choudhary, N.; Gnanamoorthy, G.; Tirth, V.; Prasad, S.; Khan, A.H.; Islam, S.; Khan, N.A. The Processing of Calcium Rich Agricultural and Industrial Waste

- for Recovery of Calcium Carbonate and Calcium Oxide and Their Application for Environmental Cleanup: A Review. *Appl. Sci.* **2021**, *11*, 4212, <http://doi.org/10.3390/app11094212>.
3. Simoni, M.; Wilkes, M.D.; Brown, S.; Provis, J.L.; Kinoshita, H.; Hanein, T. Decarbonising the lime industry: State-of-the-art. *Renew. Sustain. Energy Rev.* **2022**, *168*, 112765, <http://doi.org/10.1016/j.rser.2022.112765>.
  4. Dölle, K. In-Situ Precipitated Calcium Carbonate Paper Filler Material: A Review. *J. Eng. Res. Rep.* **2021**, *21*, 38–58, <http://doi.org/10.9734/jerr/2021/v21i1117502>.
  5. Jeon, C.W.; Park, S.; Bang, J.-H.; Chae, S.; Song, K.; Lee, S.-W. Nonpolar Surface Modification Using Fatty Acids and Its Effect on Calcite from Mineral Carbonation of Desulfurized Gypsum. *Coatings* **2018**, *8*, 43, <http://doi.org/10.3390/coatings8010043>.
  6. Azkiya, N.I.; Prasetia, F.; Putri, E.D.; Rosiana, A.; Wardhani, S. Sintesis Precipitated Calcium Carbonate (PCC) dari Batuan Kapur Alam dengan Metode Kaustik Soda (Kajian Konsentrasi HNO<sub>3</sub>), *J. Ilmu Dasar*, **2016**, *17*, 31-34.
  7. Farrag, N.M.; Bayoumi, R.A.; Mohamed, T.A. Factorial analysis of nano-precipitated calcium carbonate via a carbonation route using Solvay wastewater. *Case Stud. Chem. Environ. Eng.* **2022**, *6*, 100236, <http://doi.org/10.1016/j.csee.2022.100236>.
  8. Lunstrum, A.; Berelson, W. CaCO<sub>3</sub> dissolution in carbonate-poor shelf sands increases with ocean acidification and porewater residence time. *Geochim. Cosmochim. Acta* **2022**, *329*, 168–184, <http://doi.org/10.1016/j.gca.2022.04.031>.
  9. Dafchahi, M.N.; Resalati, H.; Zabihzadeh, S.M.; Nazarnezhad, N.; Asadpour, G.; Pirayesh, H. Novel calcium carbonate filler for cellulose industry. *Nord. Pulp Paper Res. J.* **2021**, *36*, 536–547, <http://doi.org/10.1515/npprj-2021-0018>.
  10. Dölle, K.; Bajrami, B. In Situ Precipitated Calcium Carbonate in the Presence of Pulp Fibers – A Beating Study. *J. Eng. Res. Rep.* **2021**, *20*, 1–17, <http://doi.org/10.9734/jerr/2021/v20i817352>.
  11. Ribeiro, G.D.; Hiranobe, C.T.; da Silva, J.F.R.; Torres, G.B.; Paim, L.L.; Job, A.E.; Cabrera, F.C.; dos Santos, R.J. Physical-Mechanical Properties of Chartwell® Coupling Agent-Treated Calcium Carbonate and Silica-Reinforced Hybrid Natural Rubber Composites. *Crystals* **2022**, *12*, 1552, <http://doi.org/10.3390/cryst12111552>.
  12. Ersoy, O.; Güler, D.; Rençberoglu, M. Effects of Grinding Aids Used in Grinding Calcium Carbonate (CaCO<sub>3</sub>) Filler on the Properties of Water-Based Interior Paints. *Coatings* **2022**, *12*, 44, <http://doi.org/10.3390/coatings12010044>.
  13. Peng, Y.; Musah, M.; Via, B.; Wang, X. Calcium Carbonate Particles Filled Homopolymer Polypropylene at Different Loading Levels: Mechanical Properties Characterization and Materials Failure Analysis. *J. Compos. Sci.* **2021**, *5*, 302, <http://doi.org/10.3390/jcs5110302>.
  14. Jeon, C.W.; Park, S.; Bang, J.-H.; Chae, S.; Song, K.; Lee, S.-W. Nonpolar Surface Modification Using Fatty Acids and Its Effect on Calcite from Mineral Carbonation of Desulfurized Gypsum. *Coatings* **2018**, *8*, 43, <http://doi.org/10.3390/coatings8010043>.
  15. Shin, H.Y.; Lee, J.H.; Kim, J.-Y. Formation mechanism of nanocomposites between starch and stearic acid via nanoprecipitation. *Food Hydrocoll.* **2022**, *131*, 107780, <http://doi.org/10.1016/j.foodhyd.2022.107780>.
  16. Li, J.; Wang, Y.; Gao, R.; Zhang, T.C.; Yuan, S. Superhydrophobic copper foam modified with hierarchical stearic acid/CuSiO<sub>3</sub>/Cu(OH)<sub>2</sub> nanocomposites for efficient water/oil separation. *J. Environ. Chem. Eng.* **2022**, *10*, 107618, <http://doi.org/10.1016/j.jece.2022.107618>.
  17. Sbardella, F.; Rivilla, I.; Bavasso, I.; Russo, P.; Vitiello, L.; Tirillò, J.; Sarasini, F. Zinc oxide nanostructures and stearic acid as surface modifiers for flax fabrics in polylactic acid biocomposites. *Int. J. Biol. Macromol.* **2021**, *177*, 495–504, <http://doi.org/10.1016/j.ijbiomac.2021.02.171>.
  18. Tran, H.V.; Tran, L.D.; Vu, H.D.; Thai, H. Facile surface modification of nanoprecipitated calcium carbonate by adsorption of sodium stearate in aqueous solution. *Colloids Surf. A Physicochem. Eng. Asp.* **2010**, *366*, 95–103, <http://doi.org/10.1016/j.colsurfa.2010.05.029>.
  19. Tang, Y.; Cai, Y.; Wang, L.; Luo, X.; Wang, B.; Song, Q.; Liu, Z. Formation mechanism of superhydrophobicity of stainless steel by laser-assisted decomposition of stearic acid and its corrosion resistance, *Opt. Laser Technol.* **2022**, *153*, 108190, <http://doi.org/10.1016/j.optlastec.2022.108190>.
  20. Wang, C.; Sheng, Y.; Zhao, X.; Pan, Y.; Hari-Bala; Wang, Z. Synthesis of hydrophobic CaCO<sub>3</sub> nanoparticles. *Mater. Lett.* **2006**, *60*, 854–857, <http://doi.org/10.1016/j.matlet.2005.10.035>.

21. Li, Z.; Bai, L.; Xing, Z.; Yang, W.; Wu, Q.; Zhang, G. Stearic acid-TiO<sub>2</sub> composite Janus sheets perpendicular to the interface for emulsification and photocatalysis. *Inorg. Chem. Commun.* **2022**, *144*, 109835, <http://doi.org/10.1016/j.inoche.2022.109835>.
22. Bian, Y.; Wang, K.; Wang, J.; Yu, Y.; Liu, M.; Lv, Y. Preparation and properties of capric acid: Stearic acid/hydrophobic expanded perlite-aerogel composite phase change materials. *Renew. Energy* **2021**, *179*, 1027–1035, <http://doi.org/10.1016/j.renene.2021.07.125>.
23. Patti, A.; Lecocq, H.; Serghei, A.; Acierno, D.; Cassagnau, P. The universal usefulness of stearic acid as surface modifier: applications to the polymer formulations and composite processing. *J. Ind. Eng. Chem.* **2021**, *96*, 1–33, <http://doi.org/10.1016/j.jiec.2021.01.024>.
24. Gomes, D.J.C.; de Souza, N.C.; Silva, J.R. Using a monocular optical microscope to assemble a wetting contact angle analyser. *Measurement* **2013**, *46*, 3623–3627, <http://doi.org/10.1016/j.measurement.2013.07.010>.
25. Liang, Y.; Yu, K.; Zheng, Q.; Xie, J.; Wang, T.-J. Thermal treatment to improve the hydrophobicity of ground CaCO<sub>3</sub> particles modified with sodium stearate. *Appl. Surf. Sci.* **2018**, *436*, 832–838, <http://doi.org/10.1016/j.apsusc.2017.12.023>.
26. Ukrainczyk, M.; Kontrec, J.; Kralj, D. Precipitation of different calcite crystal morphologies in the presence of sodium stearate. *J. Colloid Interface Sci.* **2009**, *329*, 89–96, <http://doi.org/10.1016/j.jcis.2008.09.045>.
27. Zaliman, S.Q.; Zakaria, N.A.; Ahmad, A.L.; Leo, C.P. 3D-imprinted superhydrophobic polyvinylidene fluoride membrane contactor incorporated with CaCO<sub>3</sub> nanoparticles for carbon capture. *Sep. Purif. Technol.* **2022**, *287*, 120519, <http://doi.org/10.1016/j.seppur.2022.120519>.
28. Zhang, Y.; Chong, J.Y.; Xu, R.; Wang, R. Hydrophobic ceramic membranes fabricated via fatty acid chloride modification for solvent resistant membrane distillation (SR-MD). *J. Membr. Sci.* **2022**, *658*, 120715, <http://doi.org/10.1016/j.memsci.2022.120715>.
29. Syafiq, A.; Vengadaesvaran, B.; Ahmed, U.; Rahim, N.A.; Pandey, A.K.; Bushroa, A.R.; Ramesh, K.; Ramesh, S. Facile synthesise of transparent hydrophobic nano-CaCO<sub>3</sub> based coatings for self-cleaning and anti-fogging. *Mater. Chem. Phys.* **2020**, *239*, 121913, <http://doi.org/10.1016/j.matchemphys.2019.121913>.
30. Wu, M.-N.; Maity, J.P.; Bundschuh, J.; Li, C.-F.; Lee, C.-R.; Hsu, C.-M.; Lee, W.-C.; Huang, C.-H.; Chen, C.-Y. Green technological approach to synthesis hydrophobic stable crystalline calcite particles with one-pot synthesis for oil–water separation during oil spill cleanup. *Water Res.* **2017**, *123*, 332–344, <http://doi.org/10.1016/j.watres.2017.06.040>.